Human Molecular Genetics, 2008, Vol. 17, No. 10 ***1349–1362***
doi:10.1093/hmg/ddn023
Advance Access published on January 25, 2008

Variations in the progranulin gene affect global gene expression in frontotemporal lobar degeneration

Alice S. Chen-Plotkin[1,2,3], Felix Geser[1,2], Joshua B. Plotkin[5], Chris M. Clark[3,4,6], Linda K. Kwong[1,2], Wuxing Yuan[1,2], Murray Grossman[3], Vivianna M. Van Deerlin[1,2], John Q. Trojanowski[1,2] and Virginia M.-Y. Lee[1,2,*]

[1]Center for Neurodegenerative Disease Research, Department of Pathology and Laboratory Medicine, [2]Institute on Aging, [3]Department of Neurology and [4]Alzheimer's Disease Center, University of Pennsylvania School of Medicine, Philadelphia, PA 19104, USA, [5]Department of Biology and [6]Center of Excellence for Research on Neurodegenerative Diseases, University of Pennsylvania, Philadelphia, PA 19104, USA

Received October 23, 2007; Revised and Accepted January 17, 2008

Frontotemporal lobar degeneration is a fatal neurodegenerative disease that results in progressive decline in behavior, executive function and sometimes language. Disease mechanisms remain poorly understood. Recently, however, the DNA- and RNA-binding protein TDP-43 has been identified as the major protein present in the hallmark inclusion bodies of frontotemporal lobar degeneration with ubiquitinated inclusions (FTLD-U), suggesting a role for transcriptional dysregulation in FTLD-U pathophysiology. Using the Affymetrix U133A microarray platform, we profiled global gene expression in both histopathologically affected and unaffected areas of human FTLD-U brains. We then characterized differential gene expression with biological pathway analyses, cluster and principal component analyses, and subgroup analyses based on brain region and progranulin (*GRN*) gene status. Comparing 17 FTLD-U brains to 11 controls, we identified 414 upregulated and 210 downregulated genes in frontal cortex (*P*-value < 0.001). Moreover, cluster and principal component analyses revealed that samples with mutations or possibly pathogenic variations in the *GRN* gene (*GRN*+, 7/17) had an expression signature that was distinct from both normal controls and FTLD-U samples lacking *GRN* gene variations (*GRN*-, 10/17). Within the subgroup of *GRN*+ FTLD-U, we found >1300 dysregulated genes in frontal cortex (*P*-value < 0.001), many participating in pathways uniquely dysregulated in the *GRN*+ cases. Our findings demonstrate a distinct molecular phenotype for *GRN*+ FTLD-U, not readily apparent on clinical or histopathological examination, suggesting distinct pathophysiological mechanisms for *GRN*+ and *GRN*- subtypes of FTLD-U. In addition, these data from a large number of human brains provide a valuable resource for future testing of disease hypotheses.

INTRODUCTION

Frontotemporal lobar degeneration (FTLD) is the second most common cause of dementia in individuals below the age of 65 years (1), with devastating effects on patients and families. Several clinical classification schemes for FTLD exist (2–4), but in general individuals suffer progressive atrophy of their frontal and temporal lobes, with corresponding deficits in the domains of behavior, social and executive function, and/or language. Pathologically, FTLD can be divided into those cases which have tau-positive inclusions (FTLD-tau) and those which are tau- and alpha-synuclein-negative but show ubiquitinated inclusions (FTLD-U), with rare cases exhibiting neither tau-positive nor ubiquitin-positive inclusions (5,6).

*To whom correspondence should be addressed to: Center for Neurodegenerative Disease Research, Department of Pathology and Laboratory Medicine, University of Pennsylvania School of Medicine, 3rd Floor Maloney, 3600 Spruce Street Philadelphia, PA 19104, USA.
Tel: +1 2156624474; Fax: +1 2153495909; Email: vmylee@mail.med.upenn.edu

Table 1. Human brain samples analyzed by microarray

	Control	All FTLD-U	GRN+ FTLD-U	GRN− FTLD-U	Total
Total cases	11	17	7	10	28
Male	7	7	3	4	14
Female	4	10	4	6	14
Median Age (IQR)	67 (54–75)	69 (59–75)	71 (67–77)	64 (53–72)	
Median PMI (IQR)	7 (5–14.5)	6 (4–9.5)	6 (5–7)	7.5 (3–11)	
Total samples	18	42	16	26	60
Cerebellum	8	13	5	8	21
Frontal cortex	8	16	6	10	24
Hippocampus	2	13	5	8	15

PMI, postmortem interval; IQR, interquartile range (25th–75th percentile).
Age, sex and PMI were not significantly different between cases and controls by a Mann–Whitney test. *GRN*+ FTLD-U includes all cases with progranulin gene abnormalities (mutations and variants), while *GRN*− FTLD-U denotes cases without progranulin gene abnormalities.

FTLD-U is the most commonly seen pathology (7), and recent advances have led to a greater understanding of FTLD-U pathophysiology at a protein and gene level. In 2006, two groups demonstrated that mutations in the gene progranulin (*GRN*) were associated with many cases of FTLD-U (8,9). Most of the *GRN* mutations found thus far result in premature termination (8–10), and protein haploinsuffiency has been suggested as a mechanism of disease (8–11). The major protein in the hallmark ubiquitinated inclusions of FTLD-U was subsequently identified as TAR DNA binding protein 43 (TDP-43), encoded by the gene *TARDBP* (12). Very recently, progranulin depletion has been shown to increase caspase-dependent cleavage of TDP-43 in an *in vitro* model, offering a possible mechanism to link these two disease-associated abnormalities (13). Strikingly, TDP-43 appears to be the major protein within the pathological inclusions of frontotemporal dementia with motor neuron disease (FTD-MND) and sporadic amyotrophic lateral sclerosis (ALS) as well (12,14–17), lending support to the view that these diseases are part of a clinicopathological spectrum (18).

With the advent of TDP-43 immunostaining, different histopathological subtypes of FTLD-U are increasingly being recognized (6,17,19). Within these subtypes, *GRN* mutations are found mainly, possibly exclusively, among a subtype (Sampathu Type 3) characterized by numerous neuronal cytoplasmic inclusions, short dystrophic neurites and a variable number of neuronal intranuclear inclusions in the superficial cortical layers (19). However, while *GRN* mutations are found in Type 3 cases, not all Type 3 cases carry *GRN* mutations (6,17). Clinically, *GRN* mutation cases present heterogeneously within the FTLD spectrum (10,20,21).

Although the function of the disease-associated protein TDP-43 is largely unknown, several lines of evidence point to a role in transcriptional regulation. First, TDP-43 is known to bind DNA (22,23), having first been identified in its role as a protein that binds to HIV transactive response DNA (24). Second, TDP-43 is known to bind RNA, regulating through this interaction the splicing of the cystic fibrosis transmembrane conductance regulator (25) and other genes (26). Finally, physiologic expression of TDP-43 appears to be nuclear (12,27,28), where it colocalizes with other nuclear bodies believed to function in transcription and splicing (27), and TDP-43 binds a number of heterogeneous ribonucleoproteins with well-known splicing activities (28).

The confluence of permissive technology and what is known about the biology of this disease sets the stage for a genome-wide analysis of gene expression in FTLD-U. In this study, we used microarray technology to evaluate the global gene expression of multiple regions of human FTLD-U brain, in comparison with neurologically normal controls. Our aims were (i) to identify dysregulated genes and pathways in this disease, (ii) to compare gene expression changes in neuropathologically affected (frontal cortex, hippocampus) and unaffected (cerebellum) areas of brain and (iii) to compare gene expression changes in FTLD-U cases with (*GRN*+) and without (*GRN*−) progranulin gene alterations.

We found that mRNA changes are extensive in FTLD-U. Moreover, *GRN*+ cases had a global gene expression signature that was distinct from both *GRN*- cases and controls, with over 1300 genes dysregulated in frontal cortex. Gene Ontology (GO) and Kyoto Encyclopedia of Genes and Genomes (KEGG) pathway analyses implicated some biological pathways as common to both *GRN*+ and *GRN*− cases (e.g. MAPK signaling), while others (e.g. TGF-beta signaling, cell cycle regulation) were unique to *GRN*+ cases. Taken together, our findings reveal major transcriptional changes in FTLD-U as a whole, as well as a previously unrecognized molecular signature for *GRN*+ FTLD-U.

RESULTS

Identification of genes differentially expressed in FTLD-U cases compared to controls

We examined global gene expression in 17 human FTLD-U brains and 11 age- and sex-matched controls (Table 1). Analyses included tissue dissected from the frontal cortex and hippocampus (regions showing significant histopathology in disease) and cerebellum (region with little histopathology in disease). We compared FTLD-U cases with controls, treating each brain region separately and controlling for age and gender. FTLD-U frontal cortex exhibited a greater number of differentially expressed transcripts relative to controls, while FTLD-U cerebellum had many fewer differentially

Table 2. mRNA changes in human FTLD-U brain—by brain region and progranulin status

	Samples	Overall probes	Increased in disease	Decreased in disease	FDR (%)
FTLD-U versus normal					
Frontal cortex	16 versus 8	624 (185)	414 (142)	210 (43)	4
Cerebellum	10 versus 7	70 (8)	28 (3)	42 (5)	27.2
GRN+ FTLD-U versus Normal					
Frontal cortex	6 versus 8	1311 (772)	579 (284)	732 (488)	1.9
Cerebellum	4 versus 7	50 (15)	25 (3)	25 (12)	39.4
GRN- FTLD-U versus Normal					
Frontal cortex	10 versus 8	154 (40)	94 (33)	60 (7)	13.8
Cerebellum	6 versus 7	218 (86)	171 (60)	47 (26)	8.7

Numbers reflect probe sets with differential expression (overall probes), increased expression in FTLD-U (increased in disease) or decreased expression in FTLD-U (decreased in disease) at $P < 0.001$. The total number meeting this statistical threshold is shown, while the number of probes meeting both a $P < 0.001$ criterion and fold change >2 criterion appears in parentheses.
FDR, false discovery rate. Determined by class permutation analysis (similar results were obtained with calculations based on nominal *P*-value). *GRN*+ FTLD-U=FTLD-U cases with progranulin gene abnormalities. *GRN*− FTLD-U=FTLD-U cases without progranulin gene abnormalities.

expressed genes, consistent with patterns of histopathology. Because of a paucity of hippocampal control samples, we could not make a statistically meaningful comparison between disease and control among the hippocampal samples.

In FTLD-U frontal cortex (16 FTLD-U, 8 controls), 624 probe sets representing 536 genes demonstrated significant differential expression at a *P*-value of 0.001 (Table 2). Of these, 414 probe sets were increased in disease, while 210 were decreased in disease. In FTLD-U cerebellum (10 FTLD-U, 7 controls), in contrast, only 70 probe sets representing 75 genes demonstrated significant differential expression at a *P*-value of 0.001. (Some probes recognized more than one gene.) To correct for multiple hypothesis testing, false discovery rates (FDR) were calculated for each comparison (Table 2). Of the 624 probe sets differentially expressed in FTLD-U frontal cortex, only 4% are expected to be false positives. In addition, to focus on genes likely to have a more significant biological effect, we imposed a minimum fold-change cutoff of two to identify genes with greater magnitudes of dysregulated expression. Applying this fold-change cutoff still resulted in our finding 185 probe sets representing 159 genes dysregulated in FTLD-U frontal cortex (Table 2). Of these, 142 transcripts were increased in disease, and 43 transcripts were decreased in disease (Supplementary Material, Table S1); the top 20 transcripts showing differential expression are summarized in Table 3.

To further evaluate the overall structure of transcriptional variation, we performed a cluster analysis of gene expression levels. Using Spearman correlation coefficients, we clustered all microarray samples across all regions and disease states in an unbiased fashion to create a hierarchical tree. With one exception, all 17 cerebellar samples regardless of disease status fell into one branch, demonstrating that these samples show different global expression from other brain regions (Fig. 1). Samples from frontal cortex and hippocampus, however, were admixed, despite the fact that cytoarchitecture in these regions is different.

If transcriptional dysregulation is a key feature of FTLD-U, one might expect more changes in gene expression in this disease than in others because of the putative nuclear transcriptional functions of TDP-43. We therefore compared the results of our study with microarray studies of other neurodegenerative diseases. Comparisons made across microarray datasets are hampered, however, by the fact that different platforms, statistical conditions and experimental conditions are used, leading to differences in statistical power and noise. To control for some of these conditions, we compared our study only with those studies using postmortem human cortical samples, with sample sizes comparable to or larger than our own frontal cortex dataset (16 disease, 8 control). We chose three representative comparison studies, one evaluating 22 disease and 9 control hippocampal samples in Alzheimer's Disease (AD, 29) one evaluating 15 disease and 5 control frontal cortex samples in sporadic Creutzfeld-Jacob Disease (sCJD, 30) and one evaluating 11 disease and 9 control motor cortex samples in sporadic ALS (31). In each case, we re-evaluated our dataset using the statistical conditions used in the comparison study, to obtain the number of genes that would be deemed to be significantly changed in a comparable analysis (Supplementary Material, Table S2). As shown in Figure 2, many more gene changes were found in the present FTLD-U study than in studies of AD or ALS; the number of dysregulated genes in FTLD-U was comparable to that seen in cases of sCJD.

In summary, many genes are differentially expressed in FTLD-U cases compared to controls. In addition, regional patterns of gene expression changes are consistent with patterns of histopathology, with frontal cortex being much more affected than cerebellum. Finally, cerebellar gene expression carries a signature distinct from that of frontal cortex or hippocampus.

Effect of progranulin gene status on global gene expression

Genetic screening of our FTLD-U cases revealed 7 cases containing progranulin gene abnormalities (*GRN*+). Of these, four possessed truncation mutations previously associated with disease and believed to be pathogenic, while the remaining three cases exhibited new variants of unknown significance (VUS, Table 4). Preliminary studies suggest that at least some of these VUS are pathogenic, and this avenue of investigation is currently ongoing. Using Spearman correlation coefficients, we clustered all frontal cortex and hippocampal

Table 3. Top 20 transcripts showing differential expression in FTLD-U

Probe ID	*P*-value	FC	Symbol	Gene
Genes showing greatest increases in expression				
209292_at	4.36E−06	4.5806	ID4	Inhibitor of DNA binding 4
204719_at	1.36E−05	4.5518	ABCA8	ATP-binding cassette, sub-family A (ABC1), member 8
221841_s_at	1.92E−05	4.2471	KLF4	Kruppel-like factor 4 (gut)
206101_at	4.23E−04	4.1557	ECM2	Extracellular matrix protein 2
209047_at	3.76E−04	4.1472	AQP1	Aquaporin 1 (Colton blood group)
205856_at	4.33E−04	4.0672	SLC14A1	Solute carrier family 14 (urea transporter)
208451_s_at	3.50E−05	4.0529	C4A/C4B	Complement component 4A
205907_s_at	4.59E−04	4.0307	OMD	Osteomodulin
211896_s_at	1.05E−04	3.8509	DCN	Decorin
205608_s_at	2.47E−06	3.6276	ANGPT1	Angiopoietin 1
209335_at	5.73E−04	3.4846	DCN	Decorin
214428_x_at	1.81E−04	3.3938	C4A/C4B	Complement component 4A
211813_x_at	2.04E−04	3.1688	DCN	Decorin
207542_s_at	3.87E−04	3.1580	AQP1	Aquaporin 1 (Colton blood group)
218418_s_at	1.36E−05	3.1493	ANKRD25	Ankyrin repeat domain 25
204457_s_at	9.84E−04	3.1478	GAS1	Growth arrest-specific 1
201893_x_at	2.23E−04	3.1145	DCN	Decorin
217678_at	4.70E−04	3.0599	SLC7A11	Solute carrier family 7
213110_s_at	5.25E−05	3.0167	COL4A5	Collagen, type IV, alpha 5 (Alport syndrome)
213592_at	8.44E−04	3.0154	AGTRL1	Angiotensin II receptor-like 1
Genes showing greatest decreases in expression				
213479_at	7.64E−04	0.1994	NPTX2	Neuronal pentraxin II
207768_at	5.95E−05	0.2053	EGR4	Early growth response 4
206115_at	2.67E−05	0.2189	EGR3	Early growth response 3
219697_at	3.09E−04	0.2375	HS3ST2	Heparan sulfate (glucosamine) 3-O-sulfotransferase 2
216086_at	1.08E−04	0.2523	SV2C	Synaptic vesicle glycoprotein 2C
211616_s_at	3.67E−04	0.2825	HTR2A	5-hydroxytryptamine (serotonin) receptor 2A
218625_at	3.67E−04	0.3156	NRN1	Neuritin 1
220794_at	1.34E−04	0.3343	GREM2	Gremlin 2, Cysteine knot superfamily
210090_at	9.41E−04	0.3535	ARC	Activity-reg cytoskeleton-associated protein
207135_at	8.85E−04	0.3617	HTR2A	5-hydroxytryptamine (serotonin) receptor 2A
205586_x_at	1.51E−04	0.3690	VGF	VGF nerve growth factor inducible
201693_s_at	9.81E−04	0.3815	EGR1	Early growth response 1
201694_s_at	4.98E−04	0.3888	EGR1	Early growth response 1
210227_at	1.49E−04	0.3997	DLGAP2	Discs, large (Drosophila) homolog-associated protein 2
206161_s_at	5.14E−04	0.4151	SYT5	Synaptotagmin V
204506_at	9.89E−04	0.4154	PPP3R1	Protein phosphatase 3 (formerly 2B), regulatory subunit B, 19 kDa, alpha isoform
205721_at	2.08E−06	0.4201	GFRA2	GDNF family receptor alpha 2
204945_at	6.75E−04	0.4223	PTPRN	Protein tyrosine phosphatase, receptor type, N
207548_at	5.98E−04	0.4246	GRM7	Glutamate receptor, metabotropic 7
214078_at	1.63E−04	0.4254	PAK3	P21 (CDKN1A)-activated kinase 3

Sixteen FTLD-U cases were compared to 8 normal controls on Affymetrix U133A microarrays. A statistical cutoff of $P < 0.001$ was used to identify genes with differential expression, which were then ranked based on fold change (FC, disease/normal). The 20 genes with largest increases (top) and decreases (bottom) in expression, identified by GeneSymbol and name, are shown for frontal cortex samples.

samples into a hierarchical dendrogram to look for any naturally arising subsets of samples. We found that almost all *GRN*+ samples (9/11), regardless of region of origin, clustered together into one branch without interspersion of *GRN*− cases of FTLD-U or control samples (Fig. 3A). This clustering result was robust to statistical methodology, seen in dendrograms produced using Pearson correlation coefficients as well.

Principal component analysis was performed as a second methodology for looking in an unbiased manner at overall data structure (Fig. 3B). Within histopathologically affected regions of brain, *GRN*+ FTLD-U cases again grouped together, defined by a low score along the first principal component (*X*-axis) and a high score along the second principal component (*Y*-axis).

Based on the observation from unbiased cluster and principal component analyses that *GRN*+ FTLD-U cases have a molecular expression signature which is distinct from *GRN*− FTLD-U cases and control subjects, we performed subgroup analyses of our gene expression data. Comparing 6 *GRN*+ frontal cortex samples to 8 normal frontal cortex samples, we found 1311 probe sets representing 1131 genes with differential expression at a *P*-value of 0.001, with an FDR of 1.9% (Table 2). Of these, 579 probe sets were increased in disease, and 732 were decreased in disease. After imposing a minimum fold change cutoff of 2, 772 probe sets representing 657 genes were still found to be differentially expressed at a *P*-value of 0.001. Of these, 284 probe sets were increased in disease, and 488 were decreased in disease (Supplementary Material, Table S3); the top 20 transcripts showing differential

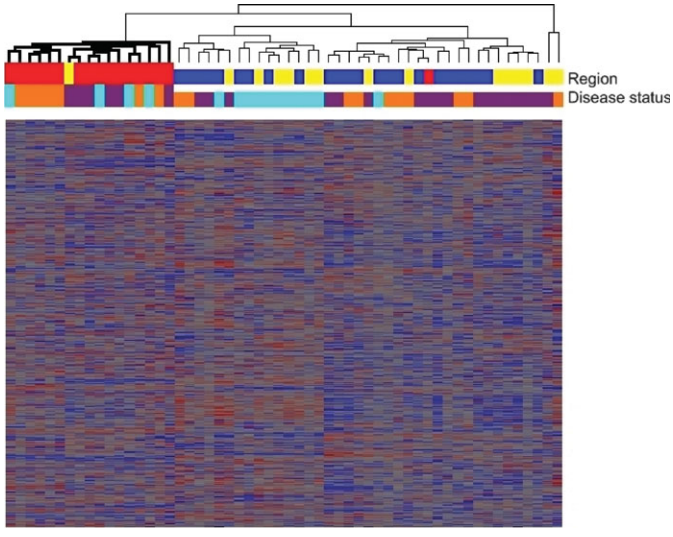

Figure 1. Cluster analysis of all samples shows a distinct expression signature for cerebellum. Hierarchical dendrogram produced by clustering of expression levels for 56 brain samples (columns) and 22 277 transcripts (rows), using Spearman correlation coefficients. With one exception, all 17 cerebellar samples (red) regardless of disease status fell into one branch (bold), while samples from frontal cortex (blue) and hippocampus (yellow) were admixed. Disease status for each sample is shown as well, with orange denoting normal cases, purple denoting FTLD-U cases without progranulin gene abnormalities (*GRN*− FTLD-U) and teal denoting FTLD-U cases with progranulin gene abnormalities (*GRN*+ FTLD-U). Heatmap tiles show standardized expression levels of individual genes with red denoting high expression, grey denoting medium expression and blue denoting low expression levels.

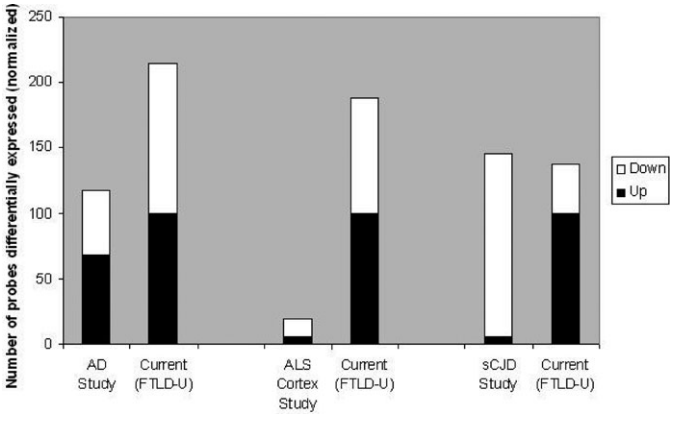

Figure 2. Number of dysregulated genes identified in human cortex microarray studies of various neurodegenerative diseases. Data from present study (FTLD-U) was re-analyzed using the same statistical conditions as each comparison study (29–31). See Supplementary Material, Table S3 for details of other studies. The black portion of each bar represents the number of upregulated genes in disease compared to control, while the white portion represents the number of downregulated genes in disease compared to control. Many more gene changes were found in the present FTLD-U study than in studies of AD or ALS.

expression are summarized in Table 5. In contrast, comparing 10 *GRN*- frontal cortex samples to 8 normal frontal cortex samples, we found only 154 probe sets representing 147 genes showing differential expression at a *P*-value of 0.001 (FDR 13.8%, Table 2). In fact, when *GRN*+ and *GRN*− frontal cortex samples were compared directly, more genes were found to be differentially expressed (208 probe sets representing 214 genes—several probes recognize more than one gene) between these molecular subtypes of disease than between the *GRN*− cases and normals (Supplementary Material, Table S4).

The finding that there are many more dysregulated genes among the *GRN*+ cases is striking given the fact that the smaller number of *GRN*+ cases offers less statistical power. The large number of dysregulated genes common to this subset of cases corroborates evidence from our cluster and principal component analyses that the *GRN*+ cases have a distinct expression signature.

As with the full dataset, cerebellar samples exhibited many fewer dysregulated genes (Table 2).

Quantitative real-time QRT–PCR validation of gene changes detected on microarrays

To corroborate gene changes detected on our microarrays, we performed QRT–PCR for a subset of upregulated and downregulated genes. For all genes tested, microarray and QRT–PCR results were consistent in both *GRN*+ and *GRN*− FTLD-U cases (Fig. 4). We used ß-actin as our reference gene for normalizing gene expression levels based on microarray data showing stable expression; comparable results were obtained using cyclophilin A as an alternate reference gene (data not shown). In general, relative to QRT–PCR, microarray results tended to underestimate the magnitude of gene changes. This has been observed in other studies as well (30,32), and likely reflects the greater amount of noise around microarray measurements, with their subsequent need for normalization.

Biological pathway analysis

Using the Database for Annotation, Visualization, and Integrated Discovery (DAVID) database mining tool (Materials and Methods), we identified biological process categories significantly over-represented in *GRN*+ and *GRN*− cases of FTLD-U. We queried both the GO database and the KEGG database using all probe sets showing differential expression in frontal cortex between disease and normal at $P < 0.001$. We analyzed *GRN*+ and *GRN*- FTLD-U cases separately because of our observation that *GRN*+ cases have a distinct signature and because the strong effect of the *GRN*+ cases tended to drive overall findings within a mixed FTLD-U disease group.

The top GO and KEGG biological process categories showing over-representation in genes dysregulated in *GRN*-FTLD-U cases ($P < 0.05$) are shown in Table 6. Genes involved in the MAPK signaling pathway, which has been implicated in a number of neurodegenerative diseases (33–35), are downregulated, as are genes involved in ion transport and cell localization. Genes involved in lipid metabolism, on the other hand, appear to be upregulated in *GRN*− FTLD-U, as has been shown for AD and HD as well (29,35).

Many more biological pathways were over-represented in *GRN*+ FTLD-U (Table 7). Of these, the majority of the biological process categories were made up of genes downregulated in disease. These included all three categories

Table 4. Cases bearing progranulin gene alterations

Case	cDNA	Protein	Truncation/variant	Reference
1	c.1252C>T	R418X	Truncation	(9)
2	c.1477C>T	R493X	Truncation	(10)
3	c.348A>C	S116S	Silent variant near splice site	New
4	c.911G>A	W304X	Truncation	(10)
5	IVS708+1-+4 del GTGA	Intronic	Intronic variant at splice site	New
6[a]	c.1009C>T	Q337X	Truncation	(53)
	c.903G>A	S301S		
	c.1070C>A	P357R		
7	c.1058G>A	S353 N	Missense variant	New

FTLD-U cases bearing progranulin gene abnormalities (*GRN*+ FTLD-U) included 4 cases with truncation mutations previously associated with disease and believed to be pathogenic, as well as 3 cases with new variants of unknown significance (VUS) that are being investigated further.
[a]Case 6 possesses three separate abnormalities within the progranulin gene. In each case, cDNA numbering is based on GenBank NM_002087.2, and predicted protein numbering is based on GenPept NP_0020278.1.
cDNA, complementary DNA; New, new variant which has not been previously reported.

downregulated in *GRN*− FTLD-U (MAPK signaling, ion transport, localization), as well as many pathways which are unique to *GRN*+ FTLD-U. Among the downregulated pathways unique to *GRN*+ FTLD-U were pathways identified in other neurodegenerative disease microarray studies—synaptic transmission, calcium signaling, neurotransmitter secretion, microtubule-based movement (29,35)—as well as pathways such as axon guidance identified in proteomics studies of neurodegeneration (34).

We found eight biological processes categories upregulated in *GRN*+ FTLD-U (Table 7). These did not include lipid metabolism, which was the only biological pathway upregulated in the *GRN*− cases. As with the downregulated pathways, many biological processes found in this study had been identified in previous studies of neurodegenerative disease. These include signal transduction (including small GTPase-mediated signal transduction) and focal adhesion, identified to be dysregulated in HD (35) and AD (29), respectively, as well as regulation of actin cytoskeleton, implicated in a proteomics study of multiple neurodegenerative diseases (34). In addition, we found several specific biological pathways upregulated in this subset which may be unique to *GRN*+ FTLD-U; they have not been identified in previous microarray-based neurodegenerative disease studies or in our *GRN*− FTLD-U cases. These include the TGF-ß signaling pathway and regulation of the cell cycle.

DISCUSSION

Global mRNA expression profiling with the Affymetrix U133A microarray platform interrogated over 22 000 transcripts and detected a large number of differentially expressed genes in FTLD-U postmortem frontal cortex samples. The vast majority of these dysregulated genes were not found in cerebellum samples. This aspect of our analysis echoes previous histopathological studies, which have shown significant pathology, both by traditional methods and by TDP-43 staining, in frontal cortex but not in cerebellum (6). With respect to *GRN* status, however, this molecular phenotyping approach revealed differences which are not captured clinically or histopathologically.

A distinct expression signature for *GRN*+ FTLD-U

By cluster analysis, principal component analysis and biological pathway analysis, we found that *GRN*+ FTLD-U cases had a distinct expression signature. While there have been suggestions of clinical and pathological differences in some FTLD-U cases with *GRN* mutations (36,38,39), the overall heterogeneity of presentations makes it difficult or nearly impossible to make distinctions on clinical or histopathological grounds alone (10,20,21). The ability to detect distinct molecular phenotypes, however, may be important in identifying patient groups more responsive to targeted therapies.

It is important to note that cluster and principal component analyses revealing the distinct expression signature for *GRN*+ FTLD-U cases were performed in an unbiased manner; we did not pre-specify subgroups but rather evaluated the overall pattern of similarity in global gene expression among all samples. The fact that the *GRN* truncation mutants (four cases) formed a group with the three cases carrying *GRN* gene VUS was somewhat surprising. This finding has implications for the pathogenicity of these variants, which are under investigation now.

Notably, 2 of the 11 *GRN*+ samples were more distant in global gene expression from the other 9 samples (Fig. 3B, labeled arrows). Of these, one (Fig. 3A, arrow) was particularly distant and remained so regardless of clustering methodology. This frontal cortex sample came from a case bearing the truncation mutation R493X. The corresponding hippocampal sample from this case did cluster with the other *GRN*+ cases. On reviewing this case, we noted significant alpha-synuclein pathology in addition to TDP-43 pathology in the frontal cortex sample, which may explain the status of this case as an outlier. The R493X mutation has previously been found in multiple FTLD-U families (10). Frontotemporal dementia and primary progressive aphasia have been the associated clinical diagnoses; pathologically, cases bearing this mutation have been characterized by ubiquitin-positive intranuclear inclusions, consistent with a Sampathu Type 3 classification (10,19). Coexisting alpha-synuclein pathology has not been previously described; thus, along with the cases bearing *GRN* gene VUS, this case is also being investigated further. The other sample clustering separately from

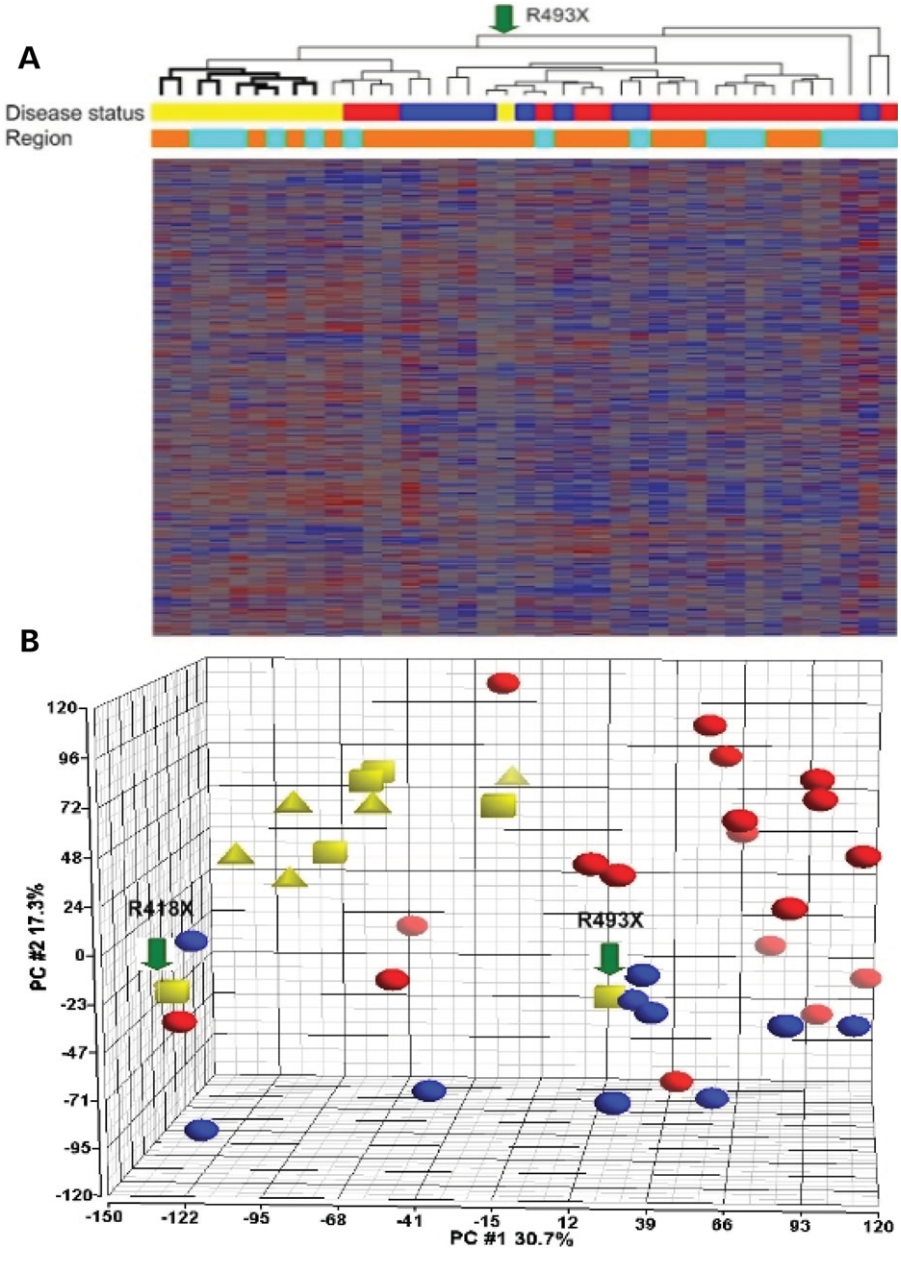

Figure 3. Cluster analysis and principal components analysis of samples from histopathologically affected brain regions show a distinct expression signature for *GRN*+ FTLD-U. (**A**) Hierarchical dendrogram produced by clustering of expression levels for 39 brain samples from frontal cortex or hippocampus (columns) and 22 277 transcripts (rows), using Spearman correlation coefficients. With two exceptions, all 11 *GRN*+ FTLD-U samples (yellow) fell into one branch (bold), while samples from *GRN*− FLTD-U (red) and normal controls (blue) were admixed. Brain region for each sample is shown as well, with orange denoting frontal cortex samples and teal denoting hippocampal samples. Heatmap tiles show standardized expression levels of individual genes with red denoting high expression, grey denoting medium expression and blue denoting low expression levels. (**B**) Principal components analysis of frontal and hippocampal samples using 22 277 transcripts also revealed a distinct expression signature for *GRN*+ FTLD-U. *GRN*+ FTLD-U samples (yellow) were characterized by a low score along the first principal component (*X*-axis) and a high score along the second principal component (*Y*-axis), separating them from *GRN*− FTLD-U samples (red) and normal samples (blue). Arrows indicate the two samples that were more distant in global gene expression by cluster analysis. Within *GRN*+ FTLD-U cases, samples bearing truncation mutations (squares) and samples bearing variants of unknown significance (triangles) were admixed. R493X=predicted protein change for indicated truncation mutant. R418X=predicted protein change for indicated truncation mutant.

the majority of the *GRN*+ FTLD-U cases is a frontal cortex sample also bearing a truncation mutation (R418X). This sample, however, appeared more related to the other *GRN*+ FTLD-U samples, with distance decreasing with the use of a parametric correlation coefficient. The corresponding hippocampal sample from this case fell into the main *GRN*+ FTLD-U cluster.

We considered various possibilities to explain our finding of a distinct *GRN*+ FTLD-U expression signature. First, this finding could be the spurious result of different treatment

Table 5. Top 20 transcripts showing differential expression in *GRN*+ FTLD-U

Probe ID	*P*-value	FC	Symbol	Gene
Genes showing greatest increases in expression				
204719_at	9.67E−05	6.3989	ABCA8	ATP-binding cassette, sub-family A (ABC1), member 8
205907_s_at	1.84E−04	6.0441	OMD	Osteomodulin
221841_s_at	1.12E−04	5.6157	KLF4	Kruppel-like factor 4 (gut)
211896_s_at	6.57E−05	5.3074	DCN	Decorin
202409_at	2.05E−04	5.3061	C11ORF43	Chromosome 11 open reading frame 43
209335_at	2.45E−04	5.1019	DCN	Decorin
209292_at	1.28E−04	5.0969	ID4	Inhibitor of DNA binding 4
206101_at	1.83E−04	5.0700	ECM2	Extracellular matrix protein 2
206373_at	8.05E−05	4.5235	ZIC1	ZIC family member 1
211742_s_at	8.28E−05	4.4841	EVI2B	Ecotropic viral integration site 2B
206100_at	3.58E−05	4.3504	CPM	Carboxypeptidase M
204457_s_at	9.77E−04	4.2875	GAS1	Growth arrest-specific 1
211813_x_at	5.88E−05	4.2649	DCN	Decorin
201893_x_at	3.97E−05	4.2531	DCN	Decorin
213975_s_at	9.53E−04	4.2301	LILRB1/LYZ	Leukocyte immunoglobulin-like receptor, subfamily B; lysozyme (renal amyloidosis)
205608_s_at	2.48E−07	4.2236	ANGPT1	Angiopoietin 1
218418_s_at	1.60E−06	4.2142	ANKRD25	Ankyrin repeat domain 25
202403_s_at	4.28E−04	4.2031	COL1A2	Collagen, type I, alpha 2
208451_s_at	1.34E−04	4.1915	C4B/C4A	Complement component 4A
203042_at	2.14E−05	4.1637	LAMP2	Lysosomal-associated membrane protein 2
Genes showing greatest decreases in expression				
221805_at	3.57E−04	0.0837	NEFL	Neurofilament, light polypeptide 68 kDa
205825_at	3.40E−04	0.0838	PCSK1	Proprotein convertase subtilisin/kexin type 1
206935_at	2.05E−05	0.0860	PCDH8	Protocadherin 8
214432_at	2.21E−04	0.1106	ATP1A3	ATPase, NA+/K+ transporting, α3 polypeptide
204337_at	4.79E−05	0.1146	RGS4	Regulator of G-protein signaling 4
203998_s_at	8.59E−04	0.1191	SYT1	Synaptotagmin I
203000_at	1.18E−04	0.1280	STMN2	Stathmin-like 2
201939_at	2.83E−05	0.1330	PLK2	Polo-like kinase 2 (Drosophila)
206115_at	2.22E−06	0.1342	EGR3	Early growth response 3
204339_s_at	1.24E−04	0.1399	RGS4	Regulator of G-protein signaling 4
206552_s_at	4.88E−04	0.1414	TAC1	Tachykinin, precursor 1 (substance K)
203999_at	4.34E−05	0.1420	SYT1	Synaptotagmin I
220359_s_at	6.21E−05	0.1433	ARPP-21	Cyclic AMP-regulated phosphoprotein, 21 kDa
206678_at	1.63E−04	0.1443	GABRA1	GABA A receptor, alpha 1
214230_at	4.53E−05	0.1454	CDC42	Cell division cycle 42 (GTP binding protein, 25 kDa)
203001_s_at	3.02E−04	0.1476	STMN2	Stathmin-like 2
201340_s_at	3.92E−04	0.1477	ENC1	Ectodermal-neural cortex
204035_at	1.68E−04	0.1490	SCG2	Secretogranin II (chromogranin C)
221916_at	1.94E−04	0.1507	NEFL	Neurofilament, light polypeptide 68 kDa
204722_at	7.20E−05	0.1540	SCN3B	Sodium channel, voltage-gated, type III, beta

Six FTLD-U cases with progranulin gene abnormalities (*GRN*+ FTLD-U) were compared to 8 normal controls on Affymetrix U133A microarrays. A statistical cutoff of $P < 0.001$ was used to identify genes with differential expression, which were then ranked based on fold change (FC, disease/normal). The 20 genes with largest increases (top) and decreases (bottom) in expression, identified by GeneSymbol and name, are shown for frontal cortex samples.

conditions for these samples. However, the 56 brain samples used in this study were collected in random order, with the operator blinded to disease and gene status. Processing of all samples after collection was performed on two consecutive days, using the same batch of microarray platforms, and the *GRN*+ samples were divided between the 2 days. Second, this finding could be the result of differing RNA quality in this subset. However, review of RNA quality parameters for these selected cases did not reveal any obvious differences from the rest of the samples. Third, while all cases in this study bearing *GRN* gene abnormalities exhibited Sampathu Type 3 histopathology (19), not all of the *GRN*− FTLD-U cases were Type 3, raising the possibility that the non-Type 3 cases drove this apparent difference in global gene expression. We therefore re-analyzed our data excluding the four *GRN*− FTLD-U cases that were not Sampathu Type 3. Excluding these cases did not materially change results (Supplementary Material, Fig. S1). Thus, we believe that the distinct global expression signature observed for *GRN*+ FTLD-U cases in this study carries biological significance.

Comparison to previous FTLD and ALS gene expression studies

While our study corroborated the findings of a previous FTLD gene expression study (40) that synapse-related genes are downregulated and cytoskeleton-associated genes are upregulated, both our experimental design and overall findings exhibited several important differences from the previous study. Because we compared affected and unaffected brain regions and also cases with and without *GRN* mutations, we were able to detect significant differences in expression levels in

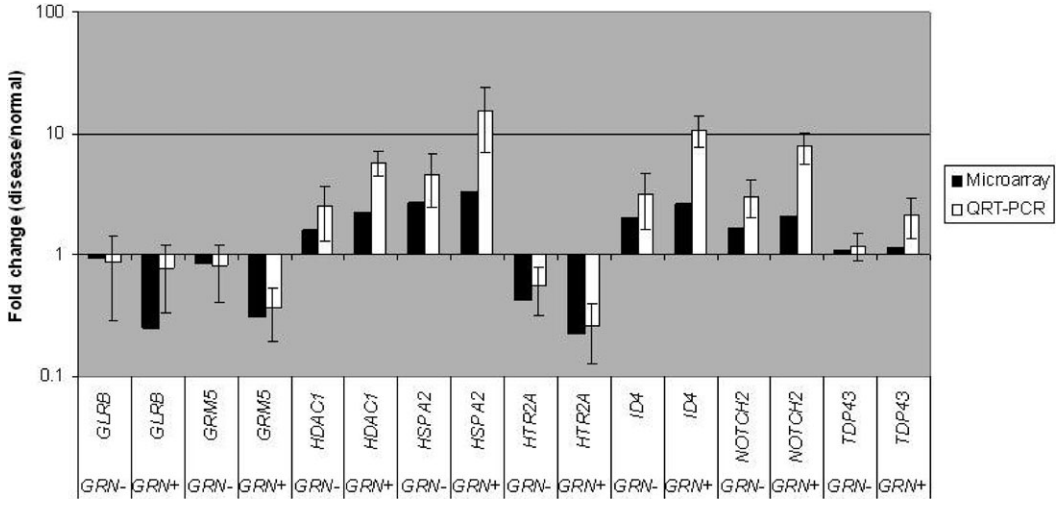

Figure 4. Validation of microarray results by quantitative reverse transcription real-time PCR (QRT–PCR). Relative expression levels of genes are indicated by the fold changes in expression level for FTLD-U samples with progranulin gene abnormalities (*GRN*+), and FTLD-U samples without progranulin gene abnormalities (*GRN*−). For QRT–PCR, average fold changes and standard deviations of three cases in each group are shown. PCR reactions were performed in duplicate. GLRB, glycine receptor beta subunit; GRM5, metabotropic glutamate receptor 5; HDAC1, histone deacetylase 1; HSPA2, heat shock protein 2 (70 kD); HTR2A, serotonin receptor 2A; ID4, inhibitor of DNA binding 4; NOTCH2, Notch homolog (Drosophila) 2.

Table 6. Dysregulated biological processes in *GRN*− FTLD-U

Database	Biological process	*P*-value	Biological process subgroups
Biological processes enriched in upregulated genes			
GO	Lipid metabolism group	2.39E−02	Cellular lipid metabolism, lipid metabolism, lipid biosynthesis, membrane lipid metabolism
Biological processes enriched in downregulated genes			
KEGG	MAPK signaling pathway	6.23E−04	
GO	Transport group	3.26E−02	Di-, tri-valent inorganic cation transport, calcium ion transport, metal ion transport, cation transport, transport, ion transport
GO	Localization group	4.78E−02	Establishment of localization, transport, localization

Frontal cortex samples from 10 FTLD-U cases without progranulin gene abnormalities (*GRN*− FTLD-U) were compared to 8 normal controls on Affymetrix U133A microarrays to identify genes with differential expression at $P < 0.001$. Biological pathway analysis using the KEGG and GO databases was then performed as described in Materials and Methods, and biological processes over-represented ($P < 0.05$) in genes upregulated in disease (top) and downregulated in disease (bottom) are shown. Biological process categories from the GO database were combined into functionally related groups, for which the median *P*-value of the subgroups is shown.

frontal cortex versus cerebellum, and in *GRN*+ cases versus *GRN*- cases relative to each other and controls. In addition, compared to the previous study, we found many more genes, involving many more biological pathways, to be dysregulated in both our FTLD-U overall group and in our *GRN*+ subset (Supplementary Material, Table S2). Fluorescent signal was present for *TARDBP* and *GRN* gene expression in all of our samples, which was not the case in the previous study (40). Finally, we found approximately equal numbers of up- and down-regulated genes for FTLD-U overall, as well as our *GRN*+ and *GRN*- subsets. In contrast, the previous study found almost all of the genes showing significant differential expression to be downregulated in disease (40).

The differing results of these two studies could reflect the fact that our study included many more samples, with greater pathological homogeneity, both of which increase statistical power.

In addition, we compared our results to a study of gene expression changes in sporadic ALS motor cortex (31) and found many more genes with differential expression (Fig. 2). In sporadic ALS, TDP-43-positive inclusions have been found in lower motor neurons (16) as well as motor cortex (37,41). These regional differences in TDP-43 histopathology and gene expression changes in FTLD-U and ALS are worthy of further examination.

Genes implicated in previous neurodegenerative disease studies

Several of the individual genes found to be dysregulated in our study have been implicated in previous studies of neurodegenerative disease. The gene found to be most downregulated in our *GRN*+ FTLD-U frontal cortex samples was the 68 kD neurofilament (NF) light polypeptide (*NEFL*), which has been associated with motor neuron disease on pathological, mouse model and human genetic grounds. Pathologically, aberrant NF accumulation has long been considered a hallmark of ALS (42). In addition, mice overexpressing *NEFL*

Table 7. Dysregulated biological processes in *GRN*+ FTLD-U

Database	Biological Process	*P*-value	Biological process subgroups
Biological processes enriched in upregulated genes			
KEGG	Focal adhesion	1.20E−02	
KEGG	TGF-beta signaling	1.32E−02	
KEGG	Regulation of actin cytoskeleton	1.60E−02	
KEGG	ECM-receptor interaction	4.53E−02	
GO	Negative regulation of biological process group	2.16E−03	Negative regulation of cellular process, negative regulation of cellular physiological process, negative regulation of biological process, negative regulation of physiological process
GO	Cell communication group	7.96E−03	Intracellular signaling cascade, signal transduction, cell communication
GO	Cell cycle group	2.69E−02	Negative regulation of progression through cell cycle, regulation of progression through cell cycle, regulation of cell cycle
GO	Small GTPase mediated signal transduction group	4.30E−02	Regulation of Ras protein signal transduction, Ras protein signal transduction, regulation of small GTPase mediated signal transduction
Biological processes enriched in downregulated genes			
KEGG	Calcium signaling pathway	1.48E−09	
KEGG	Long-term potentiation	2.32E−09	
KEGG	Gap junction	3.43E−05	
KEGG	Axon guidance	1.15E−03	
KEGG	Long-term depression	8.81E−03	
KEGG	MAPK signaling pathway	1.02E−02	
GO	Organismal physiological process/ synaptic transmission group	7.24E−08	Transmission of nerve impulse, synaptic transmission, cell–cell signaling, neurophysiological process, organismal physiological process
GO	Localization group	4.68E−05	Establishment of localization, localization, transport
GO	Secretion/transport group	1.60E−04	Neurotransmitter secretion, regulated secretory pathway, regulation of neurotransmitter levels, synaptic vesicle transport, vesicle-mediated transport, secretion, secretory pathway, synaptic vessel exocytosis, exocytosis
GO	Ion transport group	1.60E−04	Metal ion transport, cation transport, calcium ion transport, ion transport, monovalent inorganic cation transport, di-,tri-valent inorganic cation transport, potassium ion transport
GO	Cytoskeleton organization/protein polymerization group	1.56E−02	Microtubule-based movement, protein polymerization, cytoskeleton organization and biogenesis, cytoskeleton-dependent intracellular transport, microtubule-based process

Frontal cortex samples from 6 FTLD-U cases with progranulin gene abnormalities (*GRN*+ FTLD-U) were compared to 8 normal controls on Affymetrix U133A microarrays to identify genes with differential expression at $P < 0.001$. Biological pathway analysis using the KEGG and GO databases was then performed as described in Materials and Methods, and biological processes over-represented in genes upregulated in disease (top, $P < 0.05$) and downregulated in disease (bottom, $P < 0.02$) are shown. Biological Process categories from the GO database were combined into functionally related groups, for which the median *P*-value of the subgroups is shown.

(43) and mice carrying a point mutation in *NEFL* (44) show selective dysfunction and degeneration of spinal motor neurons. More recently, it has been argued that TDP-43 acts physiologically as a stabilizer of *NEFL* mRNA, with loss of this normal function involved in the pathology of FTLD-U (45). Because NFs are abundant structural components of neurons, the apparent loss of NF mRNA from postmortem samples of brain or spinal cord might be attributable simply to neuronal loss. Arguing against this, however, is the fact that we found *NEFL* mRNA expression to be downregulated only in our *GRN*+ cases. The *GRN*− FTLD-U cases, which have as much neuronal loss, did not show any differences in levels of *NEFL* mRNA expression.

GRN mutations are associated with FTLD-U, but we did not find dysregulated *GRN* mRNA expression in either our *GRN*+ or *GRN*− subsets. We considered several possible explanations. First, this result could be an artifact of combining *GRN* truncation mutants (four cases) with cases containing *GRN* gene VUS (three cases). We therefore evaluated these two categories separately but were still unable to find a statistically significant difference in *GRN* gene expression between either group and normal controls. Second, although total mRNA and protein levels of progranulin have been shown to be decreased in FTLD-U cases with *GRN* mutations (8,9), most of these studies have focused on mRNA isolated from lymphoblastoid cells rather than brain. In addition, sequencing of cDNA from brain and lymphoblastoid cells has demonstrated preferential expression of the normal allele (8,9), but this does not exclude the possibility that there is a compensatory increase in expression of the normal allele in the affected organ (brain), resulting in little difference in total mRNA levels. Third, in one case of documented decreased total mRNA expression in brain (46), *GRN* mRNA levels were decreased by ∼20% in frontal cortex and ∼10% in cerebellum; by microarray standards, such changes are relatively small and may have been below the detection level of our experimental design. Finally, the *P*-values for differential expression for the three *GRN* probe sets on our microarray platform were 0.006, 0.048 and 0.005. In an effort to detect the most robust gene changes, we may have set our statistical threshold too stringently (at $P < 0.001$) to identify this gene as significantly dysregulated. Of note, we are systematically evaluating progranulin transcript levels in different regions of human brain with QRT–PCR now and will report these findings separately.

TDP-43, the major protein found in the characteristic inclusions of FTLD-U and ALS, has been the subject of intense study recently. Initial genetic studies of TDP-43, encoded by the gene *TARDBP*, have not revealed obvious mutations within FTLD-U patients (47); mRNA expression

studies are lacking. In our microarray analysis, *TARDBP* mRNA levels were not significantly changed among either *GRN*+ or *GRN*− cases, compared to controls. There was a suggestion (Fig. 4) of slightly higher mRNA levels in the three *GRN*+ cases selected for QRT−PCR testing, but this observation remains preliminary.

Novel biological pathways in *GRN*+ FTLD-U

The present study of RNA expression profiles in human FTLD-U brain provides evidence for the commonality of some biological pathways in multiple neurodegenerative diseases. This accords with previous work implicating mechanisms such as oxidative stress (48), mitochondrial dysfunction (49), aberrant protein folding and accumulation (50), synaptic dysfunction (51) and others in several neurodegenerative diseases. Indeed, some have argued that neurodegenerative disorders are linked not just by final common pathways of cell dysfunction and death but by an actual network of interacting proteins in which abnormalities in one or a few proteins may cause dysfunction of the entire network (52,53). One recent study constructed an interacting proteomic map, with nodes representing various proteins implicated in AD, PD, ALS, HD, dentatorubropallidoluysian atrophy and prion disease (34); this map was then used to identify KEGG biological pathways enriched in disease-associated proteins. Of the 8 KEGG pathways identified in this manner, 3 (axon guidance, focal adhesion, regulation of actin cytoskeleton) were identified in our study as well, with an additional 2 (adherens junction, $P = 0.07$, Wnt signaling pathway, $P = 0.08$) falling just short of our *P*-value cutoff for significance.

Although these common pathways are important in understanding neurodegeneration as a whole, biological pathways specific to a particular disease may be key to developing targeted therapies. To that end, our study identified two biological pathways which may be specific to *GRN*+ FTLD-U. We found the categories of TGF-ß signaling and the cell cycle to be significantly enriched in genes upregulated in *GRN*+ FTLD-U. These pathways did not emerge from human brain gene expression studies of HD (35) or AD (29), general proteomics studies of neurodegeneration (34) or from analyses of our *GRN*− FTLD-U subset of cases.

Limitations of postmortem brain studies

One limitation of studies using postmortem tissue is that observed changes in gene expression may reflect either primary events in pathogenesis or secondary responses such as inflammation, cell death and neuronal loss. In addition, we used a regional sampling approach which by definition involves sampling of mixed populations of glial and neuronal cells. We chose this approach to minimize the amount of RNA degradation, which is greater with microdissection techniques. However, in doing so, we considered the possibility that primary pathophysiological changes might be masked by secondary changes of less biological importance.

Two lines of evidence from our present study support the idea that most of the genes and pathways identified have biological relevance. First, we found a distinct molecular phenotype for the *GRN*+ cases, which is unlikely to be due simply to non-specific inflammation and cell death, since the *GRN*− cases were clinically and histopathologically similar and handled the same way. Similarly, the presence of a distinct *GRN*+ FTLD-U expression signature made it unlikely that our findings are simply the result of neuronal cell loss, causing a more 'glial' signature in diseased brains, since both *GRN*+ and *GRN*− cases exhibited comparable amounts of neuronal cell loss. Second, many microarray studies have found genes involved in stress or immune response and apoptosis to be upregulated in their datasets (29,31), raising the issue of whether microarrays on postmortem tissue simply reflect the end-stage events of vulnerable cells dying. While categories of response to stress and apoptosis did appear in our biological pathway analysis, they were much less significantly enriched and did not meet our stringent statistical criterion for inclusion.

Conclusions and implications for future studies

We used a global mRNA expression profiling approach to characterize human postmortem FTLD-U brain. Our study was large, with 56 brain samples, and designed to evaluate the effect of brain region and progranulin gene status. We found many dysregulated genes within the regions of the brain affected histopathologically in disease, but not in areas which are relatively histopathologically spared. In addition, we found a distinct molecular phenotype for *GRN*+ FTLD-U, with associated biological pathways which may be specific for this subtype of disease. This finding has implications for future therapeutic strategies.

Although our study did not focus exclusively on one histopathological subtype of FTLD-U, Sampathu Type 3 FTLD-U cases (19) comprised the majority of our disease samples. We emphasized this type in order to create a balanced comparison between *GRN*+ and *GRN*− cases, since *GRN* mutations are found primarily within Type 3 cases. Future studies investigating whether the gene changes seen extend to all histopathological subtypes of FTLD-U, and to FTD-MND and ALS, would be a valuable addition to the data presented here.

Finally, the rationale for performing an RNA expression analysis in FTLD-U came from the observation that a DNA- and RNA-binding protein, TDP-43, may be involved in pathogenesis. The fact that a vast number of genes show dysregulated expression in brain regions characterized by TDP-43 pathology lends support to the idea that gene expression changes seen in FTLD-U may be more than bystander effects or lead-generating 'hits' for further analysis. If transcriptional dysregulation is a key disease mechanism in FTLD-U, these changes may be central to its pathophysiology.

MATERIALS AND METHODS

Human brain samples

Seventeen FTLD-U cases and 11 neurologically normal controls were sampled from the University of Pennsylvania Center for Neurodegenerative Disease Research Brain Bank (Table 1). Informed consent was obtained for postmortem studies. Age, sex and postmortem interval (PMI) to autopsy

were not significantly different between cases and controls. All FTLD-U cases were reviewed by a board-certified neuropathologist. In order to facilitate comparison of *GRN*+ and *GRN*− cases, the majority of the FTLD-U cases used (13/17) met criteria for FTLD-U Type 3 according to Sampathu (19). All FTLD-U cases were evaluated for abnormalities in the progranulin gene, as previously described (54). Among the FTLD-U cases, seven had progranulin gene alterations (*GRN*+), with four cases carrying known pathogenic mutations and three cases carrying VUS (Table 4). Preliminary evidence indicates that at least two of the VUS may be pathogenic by affecting mRNA splicing. Studies of these variants are in progress. All seven *GRN*+ cases met criteria for FTLD-U Type 3. Control brains had no evidence of neurological disease either clinically or neuropathologically. For each brain used, a 50–100 mg sample of frozen tissue was collected from frontal cortex grey matter anterior to the genu of the corpus callosum, cerebellum and hippocampus (where available), while keeping the brain on dry ice. Samples were either processed immediately or stored at −80°C.

RNA extraction and hybridization

Frozen tissue samples were homogenized for 30–60 s using a PowerGen 35 (Fisher Scientific). RNA was isolated using TRIzol (Invitrogen) and RNeasy Mini columns (Qiagen), according to standard manufacturer protocols. All subsequent steps were conducted as described in the Affymetrix GeneChip Expression Analysis Technical Manual (Affymetrix). Briefly, 3 μg of total RNA from each sample were used to prepare biotinylated fragmented cRNA with products from Affymetrix according to manufacturer protocols. Microarrays (Affymetrix Human Genome U133A) assessing expression of 22 277 transcripts were hybridized for 16 h at 45°C. Chips were washed and stained, and hybridization signals were collected with a GeneChip 3000 7G scanner (Affymetrix).

Microarray quality control

Measures were taken both prior to microarray hybridization and after hybridization to ensure quality control. After RNA isolation, RNA purity and integrity were assessed by spectrophotometric measurement of 260/280 nm OD ratios and by capillary electrophoresis on an Agilent 2100 Bioanalyzer. All samples used for further analysis had a 260/280 ratio of >1.9, with sharp ribosomal RNA peaks (Supplementary Material, Fig. S2), virtually undetectable low molecular weight RNA, and RIN numbers >8 (55). After microarray hybridization, 3′/5′ ratios of GAPDH were calculated, and only chips with ratios <3 were retained. Finally, we used a quality assessment algorithm based on weights and residuals from robust regression models of gene expression to identify outlier chips (56), which were excluded from analysis. Four samples were eliminated from analysis after all quality control measures; of these, two were identified by all three methods, implying that initial RNA quality may be the most important factor.

Microarray data analysis

Statistical analyses of gene expression were performed using open source R software packages available from http://www.bioconductor.org (57). Fluorescence intensity measures of gene expression were normalized and quantified by robust multi-array analysis (58), using the affy package (59). To identify transcripts differentially expressed between disease (all FTLD-U, *GRN*+ subset, *GRN*− subset) and controls for each brain region, we used the limma package (60), which adopts a Bayesian approach. Our model corrected for gender and age. FDR were calculated based on nominal *P*-values as described (35) and by using a class permutation test to adjust for co-expressed genes. R-scripts for these analyses are available on request. In addition, principal components analysis and hierarchical cluster analysis using Spearman and Pearson correlation coefficients was performed using Partek software, version 6.3 Copyright © 2007 (Partek, Inc., St Louis, MO, USA).

Biological pathway analysis

We used the DAVID 2007 program available at http://david.abcc.ncifcrf.gov/ (61) to assign differentially expressed genes to biological pathways and processes annotated in the GO and KEGG databases, available at http://www.geneontology.org (62) and http://www.genome.jp/kegg/ (63), respectively. DAVID uses a Fisher's exact test to find overrepresentation of differentially expressed genes within each biological pathway represented in the GO and KEGG databases. In addition, because of the hierarchical organization of GO categories, simple lists tend to result in similar, redundant categories. DAVID curates these GO categories into related groups based on this hierarchical structure, allowing for a more biologically meaningful analysis. We retained those pathways with a *P*-value of 0.05 or less (or, in the case of GO categories, functional groups with a median *P*-value of 0.05 or less) as statistically significant.

Quantitative RT–PCR

QRT–PCR was performed using the Applied Biosystems 7900HT Fast Real-Time PCR system. Briefly, total RNA isolated from postmortem brain samples was treated with DNAse (DNA-*free* kit; Ambion) according to manufacturer protocols, and 1.75 μg of DNAse-treated RNA was used to make single-stranded cDNA (Superscript III; Invitrogen) according to the manufacturer's protocols. One microliter of the resulting cDNA then underwent further PCR cycles, using the Taqman Gene Expression System (Applied Biosystems). PCR conditions used were 95°C for 10 min, followed by 40 cycles of denaturing at 95°C for 15 s and annealing/extension at 60°C for 1 min, in a 20 μl reaction volume. Detailed information on primer sets used is given in Supplementary Material, Table S5. The delta–delta method (64) was used for relative quantification of gene expression. We used ß-actin and cyclophilin A as our reference genes. For QRT–PCR validation of microarray results, three frontal cortex samples from each group were selected to represent the controls, *GRN*+ cases and *GRN*− cases (9 total samples).

SUPPLEMENTARY MATERIAL

Supplementary Material is available at HMG Online.

ACKNOWLEDGEMENTS

We are grateful to the Penn Microarray Facility and Dr Don Baldwin for advice and technical assistance with array samples. We thank Dr Bruce Miller for recruiting patients who were studied. Finally, we thank our patients and their families whose generosity has made this work possible.

Conflict of Interest statement: None declared.

FUNDING

These studies were supported by grants from the National Institutes of Health (NIH, AG17586, AG10124, AG15116, AG023501, AG19724 and NS44266). A.S.C.-P. is a fellow of the NINDS Morris K. Udall Parkinson's Disease Research Center of Excellence and the NIH Research Fellowship Training Program for Clinicians in Translational Research in Neurobiology of Disease. J.B.P. is supported by a Burroughs Wellcome Fund Career Award at the Scientific Interface. V.M.-Y.L. is the John H. Ware, 3rd Professor of Alzheimer's disease research. J.Q.T. is the William Maul Measey-Truman G. Schnabel, Jr Professor of Geriatric Medicine and Gerontology.

REFERENCES

1. Ratnavalli, E., Brayne, C., Dawson, K. and Hodges, J.R. (2002) The prevalence of frontotemporal dementia. *Neurology*, **58**, 1615–1621.
2. McKhann, G.M., Albert, M.S., Grossman, M., Miller, B., Dickson, D. and Trojanowski, J.Q. (2001) Clinical and pathological diagnosis of frontotemporal dementia: report of the Work Group on Frontotemporal Dementia and Pick's Disease. *Arch. Neurol.*, **58**, 1803–1809.
3. Neary, D., Snowden, J.S., Gustafson, L., Passant, U., Stuss, D., Black, S., Freedman, M., Kertesz, A., Robert, P.H., Albert, M. *et al.* (1998) Frontotemporal lobar degeneration: a consensus on clinical diagnostic criteria. *Neurology*, **51**, 1546–1554.
4. (1994) Clinical and neuropathological criteria for frontotemporal dementia. the Lund and Manchester Groups. *J. Neurol. Neurosurg. Psychiatry*, **57**, 416–418.
5. Forman, M.S., Farmer, J., Johnson, J.K., Clark, C.M., Arnold, S.E., Coslett, H.B., Chatterjee, A., Hurtig, H.I., Karlawish, J.H., Rosen, H.J. *et al.* (2006) Frontotemporal dementia: clinicopathological correlations. *Ann. Neurol.*, **59**, 952–962.
6. Cairns, N.J., Bigio, E.H., Mackenzie, I.R., Neumann, M., Lee, V.M., Hatanpaa, K.J., White, C.L., 3rd, Schneider, J.A., Grinberg, L.T., Halliday, G. *et al.* (2007) Neuropathologic diagnostic and nosologic criteria for frontotemporal lobar degeneration: consensus of the Consortium for Frontotemporal Lobar Degeneration. *Acta Neuropathol. (Berl.)*, **114**, 5–22.
7. Lipton, A.M., White, C.L., 3rd and Bigio, E.H. (2004) Frontotemporal lobar degeneration with motor neuron disease-type inclusions predominates in 76 cases of frontotemporal degeneration. *Acta Neuropathol. (Berl.)*, **108**, 379–385.
8. Cruts, M., Gijselinck, I., van der Zee, J., Engelborghs, S., Wils, H., Pirici, D., Rademakers, R., Vandenberghe, R., Dermaut, B., Martin, J.J. *et al.* (2006) Null mutations in progranulin cause ubiquitin-positive frontotemporal dementia linked to chromosome 17q21. *Nature*, **442**, 920–924.
9. Baker, M., Mackenzie, I.R., Pickering-Brown, S.M., Gass, J., Rademakers, R., Lindholm, C., Snowden, J., Adamson, J., Sadovnick, A.D., Rollinson, S. *et al.* (2006) Mutations in progranulin cause tau-negative frontotemporal dementia linked to chromosome 17. *Nature*, **442**, 916–919.
10. Gass, J., Cannon, A., Mackenzie, I.R., Boeve, B., Baker, M., Adamson, J., Crook, R., Melquist, S., Kuntz, K., Petersen, R. *et al.* (2006) Mutations in progranulin are a major cause of ubiquitin-positive frontotemporal lobar degeneration. *Hum. Mol. Genet.*, **15**, 2988–3001.
11. Pickering-Brown, S.M. (2007) Progranulin and frontotemporal lobar degeneration. *Acta Neuropathol. (Berl.)*, **114**, 39–47.
12. Neumann, M., Sampathu, D.M., Kwong, L.K., Truax, A.C., Micsenyi, M.C., Chou, T.T., Bruce, J., Schuck, T., Grossman, M., Clark, C.M. *et al.* (2006) Ubiquitinated TDP-43 in frontotemporal lobar degeneration and amyotrophic lateral sclerosis. *Science*, **314**, 130–133.
13. Zhang, Y.J., Xu, Y.F., Dickey, C.A., Buratti, E., Baralle, F., Bailey, R., Pickering-Brown, S., Dickson, D. and Petrucelli, L. (2007) Progranulin mediates caspase-dependent cleavage of TAR DNA binding protein-43. *J. Neurosci.*, **27**, 10530–10534.
14. Arai, T., Hasegawa, M., Akiyama, H., Ikeda, K., Nonaka, T., Mori, H., Mann, D., Tsuchiya, K., Yoshida, M., Hashizume, Y. *et al.* (2006) TDP-43 is a component of ubiquitin-positive tau-negative inclusions in frontotemporal lobar degeneration and amyotrophic lateral sclerosis. *Biochem. Biophys. Res. Commun.*, **351**, 602–611.
15. Cairns, N.J., Neumann, M., Bigio, E.H., Holm, I.E., Troost, D., Hatanpaa, K.J., Foong, C., White, C.L., 3rd, Schneider, J.A., Kretzschmar, H.A. *et al.* (2007) TDP-43 in familial and sporadic frontotemporal lobar degeneration with ubiquitin inclusions. *Am. J. Pathol.*, **171**, 227–240.
16. Mackenzie, I.R., Bigio, E.H., Ince, P.G., Geser, F., Neumann, M., Cairns, N.J., Kwong, L.K., Forman, M.S., Ravits, J., Stewart, H. *et al.* (2007) Pathological TDP-43 distinguishes sporadic amyotrophic lateral sclerosis from amyotrophic lateral sclerosis with SOD1 mutations. *Ann. Neurol.*, **61**, 427–434.
17. Kwong, L.K., Neumann, M., Sampathu, D.M., Lee, V.M. and Trojanowski, J.Q. (2007) TDP-43 proteinopathy: the neuropathology underlying major forms of sporadic and familial frontotemporal lobar degeneration and motor neuron disease. *Acta Neuropathol. (Berl.)*, **114**, 63–70.
18. Mackenzie, I.R. and Feldman, H.H. (2005) Ubiquitin immunohistochemistry suggests classic motor neuron disease, motor neuron disease with dementia, and frontotemporal dementia of the motor neuron disease type represent a clinicopathologic spectrum. *J. Neuropathol. Exp. Neurol.*, **64**, 730–739.
19. Sampathu, D.M., Neumann, M., Kwong, L.K., Chou, T.T., Micsenyi, M., Truax, A., Bruce, J., Grossman, M., Trojanowski, J.Q. and Lee, V.M. (2006) Pathological heterogeneity of frontotemporal lobar degeneration with ubiquitin-positive inclusions delineated by ubiquitin immunohistochemistry and novel monoclonal antibodies. *Am. J. Pathol.*, **169**, 1343–1352.
20. Mackenzie, I.R. (2007) The neuropathology and clinical phenotype of FTD with progranulin mutations. *Acta Neuropathol. (Berl.)*, **114**, 49–54.
21. Huey, E.D., Grafman, J., Wassermann, E.M., Pietrini, P., Tierney, M.C., Ghetti, B., Spina, S., Baker, M., Hutton, M., Elder, J.W. *et al.* (2006) Characteristics of frontotemporal dementia patients with a Progranulin mutation. *Ann. Neurol.*, **60**, 374–380.
22. Buratti, E. and Baralle, F.E. (2001) Characterization and functional implications of the RNA binding properties of nuclear factor TDP-43, a novel splicing regulator of CFTR exon 9. *J. Biol. Chem.*, **276**, 36337–36343.
23. Ayala, Y.M., Pantano, S., D'Ambrogio, A., Buratti, E., Brindisi, A., Marchetti, C., Romano, M. and Baralle, F.E. (2005) Human, Drosophila, and C.elegans TDP43: nucleic acid binding properties and splicing regulatory function. *J. Mol. Biol.*, **348**, 575–588.
24. Ou, S.H., Wu, F., Harrich, D., Garcia-Martinez, L.F. and Gaynor, R.B. (1995) Cloning and characterization of a novel cellular protein, TDP-43, that binds to human immunodeficiency virus type 1 TAR DNA sequence motifs. *J. Virol.*, **69**, 3584–3596.
25. Buratti, E., Dork, T., Zuccato, E., Pagani, F., Romano, M. and Baralle, F.E. (2001) Nuclear factor TDP-43 and SR proteins promote in vitro and in vivo CFTR exon 9 skipping. *EMBO J.*, **20**, 1774–1784.
26. Mercado, P.A., Ayala, Y.M., Romano, M., Buratti, E. and Baralle, F.E. (2005) Depletion of TDP 43 overrides the need for exonic and intronic splicing enhancers in the human apoA-II gene. *Nucleic Acids Res.*, **33**, 6000–6010.

27. Wang, H.Y., Wang, I.F., Bose, J. and Shen, C.K. (2004) Structural diversity and functional implications of the eukaryotic TDP gene family. *Genomics*, **83**, 130–139.
28. Buratti, E., Brindisi, A., Giombi, M., Tisminetzky, S., Ayala, Y.M. and Baralle, F.E. (2005) TDP-43 binds heterogeneous nuclear ribonucleoprotein A/B through its C-terminal tail: an important region for the inhibition of cystic fibrosis transmembrane conductance regulator exon 9 splicing. *J. Biol. Chem.*, **280**, 37572–37584.
29. Blalock, E.M., Geddes, J.W., Chen, K.C., Porter, N.M., Markesbery, W.R. and Landfield, P.W. (2004) Incipient Alzheimer's disease: microarray correlation analyses reveal major transcriptional and tumor suppressor responses. *Proc. Natl Acad. Sci. USA*, **101**, 2173–2178.
30. Xiang, W., Windl, O., Westner, I.M., Neumann, M., Zerr, I., Lederer, R.M. and Kretzschmar, H.A. (2005) Cerebral gene expression profiles in sporadic Creutzfeldt-Jakob disease. *Ann. Neurol.*, **58**, 242–257.
31. Lederer, C.W., Torrisi, A., Pantelidou, M., Santama, N. and Cavallaro, S. (2007) Pathways and genes differentially expressed in the motor cortex of patients with sporadic amyotrophic lateral sclerosis. *BMC Genomics*, **8**, 26.
32. Shi, L., Reid, L.H., Jones, W.D., Shippy, R., Warrington, J.A., Baker, S.C., Collins, P.J., de Longueville, F., Kawasaki, E.S., Lee, K.Y. *et al.* (2006) The MicroArray Quality Control (MAQC) project shows inter- and intraplatform reproducibility of gene expression measurements. *Nat. Biotechnol.*, **24**, 1151–1161.
33. Schroeter, H., Boyd, C., Spencer, J.P., Williams, R.J., Cadenas, E. and Rice-Evans, C. (2002) MAPK signaling in neurodegeneration: influences of flavonoids and of nitric oxide. *Neurobiol. Aging*, **23**, 861–880.
34. Limviphuvadh, V., Tanaka, S., Goto, S., Ueda, K. and Kanehisa, M. (2007) The commonality of protein interaction networks determined in Neurodegenerative disorders (NDDs). *Bioinformatics*, **23**, 2129–2138.
35. Hodges, A., Strand, A.D., Aragaki, A.K., Kuhn, A., Sengstag, T., Hughes, G., Elliston, L.A., Hartog, C., Goldstein, D.R., Thu, D. *et al.* (2006) Regional and cellular gene expression changes in human Huntington's disease brain. *Hum. Mol. Genet.*, **15**, 965–977.
36. Davion, S., Johnson, N., Weintraub, S., Mesulam, M.M., Engberg, A., Mishra, M., Baker, M., Adamson, J., Hutton, M., Rademakers, R. *et al.* (2007) Clinicopathologic correlation in PGRN mutations. *Neurology*, **69**, 1113–1121.
37. Geser, F., Brandmeir, N., Kwong, L., Martinez-Lage, M., Elman, L., McCluskey, L., Xie, S., Lee, V. and Trojanowski, J. (2008) Whole brain map of pathological TDP-43 in amyotrophic lateral sclerosis suggests a multisystem disorder. *Arch. Neurol.*, in press.
38. Mackenzie, I.R., Baker, M., Pickering-Brown, S., Hsiung, G.Y., Lindholm, C., Dwosh, E., Gass, J., Cannon, A., Rademakers, R., Hutton, M. *et al.* (2006) The neuropathology of frontotemporal lobar degeneration caused by mutations in the progranulin gene. *Brain*, **129**, 3081–3090.
39. Snowden, J.S., Pickering-Brown, S.M., Mackenzie, I.R., Richardson, A.M., Varma, A., Neary, D. and Mann, D.M. (2006) Progranulin gene mutations associated with frontotemporal dementia and progressive non-fluent aphasia. *Brain*, **129**, 3091–3102.
40. Mishra, M., Paunesku, T., Woloschak, G.E., Siddique, T., Zhu, L.J., Lin, S., Greco, K. and Bigio, E.H. (2007) Gene expression analysis of frontotemporal lobar degeneration of the motor neuron disease type with ubiquitinated inclusions. *Acta Neuropathol. (Berl.)*, **114**, 81–94.
41. Tan, C.F., Eguchi, H., Tagawa, A., Onodera, O., Iwasaki, T., Tsujino, A., Nishizawa, M., Kakita, A. and Takahashi, H. (2007) TDP-43 immunoreactivity in neuronal inclusions in familial amyotrophic lateral sclerosis with or without SOD1 gene mutation. *Acta Neuropathol. (Berl.)*, **113**, 535–542. Epub 2007 Feb 27.
42. Hirano, A., Donnenfeld, H., Sasaki, S. and Nakano, I. (1984) Fine structural observations of neurofilamentous changes in amyotrophic lateral sclerosis. *J. Neuropathol. Exp. Neurol.*, **43**, 461–470.
43. Xu, Z., Cork, L.C., Griffin, J.W. and Cleveland, D.W. (1993) Increased expression of neurofilament subunit NF-L produces morphological alterations that resemble the pathology of human motor neuron disease. *Cell*, **73**, 23–33.
44. Lee, M.K., Marszalek, J.R. and Cleveland, D.W. (1994) A mutant neurofilament subunit causes massive, selective motor neuron death: implications for the pathogenesis of human motor neuron disease. *Neuron*, **13**, 975–988.
45. Strong, M.J., Volkening, K., Hammond, R., Yang, W., Strong, W., Leystra-Lantz, C. and Shoesmith, C. (2007) TDP43 is a human low molecular weight neurofilament (hNFL) mRNA-binding protein. *Mol. Cell. Neurosci.*, **35**, 320–327.
46. Leverenz, J.B., Yu, C.E., Montine, T.J., Steinbart, E., Bekris, L.M., Zabetian, C., Kwong, L.K., Lee, V.M., Schellenberg, G.D. and Bird, T.D. (2007) A novel progranulin mutation associated with variable clinical presentation and tau, TDP43 and alpha-synuclein pathology. *Brain*, **130**, 1360–1374.
47. Rollinson, S., Snowden, J.S., Neary, D., Morrison, K.E., Mann, D.M. and Pickering-Brown, S.M. (2007) TDP-43 gene analysis in frontotemporal lobar degeneration. *Neurosci. Lett.*, **419**, 1–4.
48. Andersen, J.K. (2004) Oxidative stress in neurodegeneration: cause or consequence? *Nat. Med.*, **10** (Suppl.), S18–S25.
49. Lin, M.T. and Beal, M.F. (2006) Mitochondrial dysfunction and oxidative stress in neurodegenerative diseases. *Nature*, **443**, 787–795.
50. Lansbury, P.T. and Lashuel, H.A. (2006) A century-old debate on protein aggregation and neurodegeneration enters the clinic. *Nature*, **443**, 774–779.
51. Bossy-Wetzel, E., Schwarzenbacher, R. and Lipton, S.A. (2004) Molecular pathways to neurodegeneration. *Nat. Med.*, **10** (Suppl.), S2–S9.
52. Lim, J., Hao, T., Shaw, C., Patel, A.J., Szabo, G., Rual, J.F., Fisk, C.J., Li, N., Smolyar, A., Hill, D.E. *et al.* (2006) A protein–protein interaction network for human inherited ataxias and disorders of Purkinje cell degeneration. *Cell*, **125**, 801–814.
53. Fraser, H.B. (2006) Coevolution, modularity and human disease. *Curr. Opin. Genet. Dev.*, **16**, 637–644.
54. Van Deerlin, V., Wood, E. and Moore, P. (2007) Clinical, genetic, and pathological characteristics of patients with frontotemporal dementia and progranulin mutations. *Arch. Neurol.*, **64**, 1148–1153.
55. Schroeder, A., Mueller, O., Stocker, S., Salowsky, R., Leiber, M., Gassmann, M., Lightfoot, S., Menzel, W., Granzow, M. and Ragg, T. (2006) The RIN: an RNA integrity number for assigning integrity values to RNA measurements. *BMC Mol. Biol.*, **7**, 3.
56. Bolstad, B.M., Collin, F., Simpson, K.M., Irizarry, R.A. and Speed, T.P. (2004) Experimental design and low-level analysis of microarray data. *Int. Rev. Neurobiol.*, **60**, 25–58.
57. Gentleman, R.C., Carey, V.J., Bates, D.M., Bolstad, B., Dettling, M., Dudoit, S., Ellis, B., Gautier, L., Ge, Y., Gentry, J. *et al.* (2004) Bioconductor: open software development for computational biology and bioinformatics. *Genome Biol.*, **5**, R80.
58. Irizarry, R.A., Bolstad, B.M., Collin, F., Cope, L.M., Hobbs, B. and Speed, T.P. (2003) Summaries of Affymetrix GeneChip probe level data. *Nucleic Acids Res.*, **31**, e15.
59. Gautier, L., Cope, L., Bolstad, B.M. and Irizarry, R.A. (2004) Affy—analysis of Affymetrix GeneChip data at the probe level. *Bioinformatics*, **20**, 307–315.
60. Smyth, G.K. (2004) Linear models and empirical bayes methods for assessing differential expression in microarray experiments. *Stat. Appl. Genet. Mol. Biol.*, **3**, Article 3.
61. Dennis, G., Jr, Sherman, B.T., Hosack, D.A., Yang, J., Gao, W., Lane, H.C. and Lempicki, R.A. (2003) DAVID: database for annotation, visualization, and integrated discovery. *Genome Biol.*, **4**, P3.
62. Ashburner, M., Ball, C.A., Blake, J.A., Botstein, D., Butler, H., Cherry, J.M., Davis, A.P., Dolinski, K., Dwight, S.S., Eppig, J.T. *et al.* (2000) Gene ontology: tool for the unification of biology. The Gene Ontology Consortium. *Nat. Genet.*, **25**, 25–29.
63. Kanehisa, M., Goto, S., Hattori, M., Aoki-Kinoshita, K.F., Itoh, M., Kawashima, S., Katayama, T., Araki, M. and Hirakawa, M. (2006) From genomics to chemical genomics: new developments in KEGG. *Nucleic Acids Res.*, **34**, D354–D357.
64. Livak, K.J. and Schmittgen, T.D. (2001) Analysis of relative gene expression data using real-time quantitative PCR and the 2(-Delta Delta C(T)) Method. *Methods*, **25**, 402–408.